Robust Decentralized Design of H_∞-based Frequency Stabilizer of SMES

www.serd.ait.ac.th/reric

C. Vorakulpipat [*], M. Leelajindakrirerk [*], and I. Ngamroo [**]

[*] Electrical Engineering Department
King Mongkut's Institute of Technology
Ladkrabang, Bangkok

[**] Electrical Power Engineering Program
Sirindhorn International Institute of Technology
Thammasat University, Pathumtani
THAILAND

ABSTRACT

This paper presents a new robust decentralized design of frequency stabilizer for superconducting magnetic energy storage (SMES) based on an H_∞ control. As an interconnected power system is subjected to load disturbances, system frequency may be severely disturbed and oscillate. To stabilize frequency oscillations, the active power control by SMES installed in a power system can be applied. The proposed decentralized control design translates interconnected power systems installed with SMESs into a Multi-Input Multi-Output (MIMO) control system. The technique of overlapping decompositions is applied to extract the decoupled subsystem with Single-Input Single-Output (SISO) from an MIMO system. As a result, a frequency stabilizer of SMES can be independently designed to enhance the damping of the inter-area mode embedded in the decoupled subsystem. In addition, to guarantee the robust stability of system against uncertainties such as system parameters variations etc., the multiplicative uncertainty model is also incorporated. Consequently, H_∞ control via a mixed sensitivity approach is applied to design the robust frequency stabilizer of SMES. Study results explicitly show that the robustness of the H_∞-based frequency stabilizer of SMES is superior to that of the PID based stabilizer under various load disturbances and negative damping.

1. INTRODUCTION

Nowadays, various kinds of apparatus with large power consumption, such as, a magnetic levitation transportation, a large scale accelerator, a testing plant for nuclear fusion etc., tend to increase significantly. When these loads are concentrated in an interconnected power system, they may cause a serious problem of frequency oscillation. Especially, if the frequency of changing load is in the vicinity of the inter-area oscillation mode (0.2-0.8 Hz), the oscillation of system frequency may experience a serious stability problem due to an inadequate damping. Under this situation, the conventional frequency control, i.e. a governor, may no longer be able to absorb the large frequency oscillations due to its slow response [1]. In order to compensate these sudden load changes and stabilize frequency oscillation, an active power source with fast response, such as SMES [2], is expected as one of the most effective countermeasure.

In the literature [3-5], a SMES is proposed for investigating its application to frequency control. It has been observed that a SMES can effectively reduce frequency and tie-line power oscillations following sudden load disturbances. Nevertheless, system uncertainties such as changes in system configuration due to unpredictable disturbance, system parameters variation and modeling errors, etc. have not been considered in these literatures. The frequency stabilizer of SMES that are designed without taking system uncertainties into consideration may not guarantee a robust stability of the system.

To solve this problem, this paper proposes a new robust decentralized design of frequency stabilizers for SMESs based on an H_∞ control. The multiplicative uncertainty model is employed to represent all possible uncertainties in interconnected power systems. The H_∞ control based on mixed sensitivity approach is applied to design frequency stabilizer. The robustness of designed frequency stabilizer is evaluated in the three-area loop interconnected system.

The organization of this paper is as follows. Section 2 provides the motivation of the proposed control. Next, Section 3 explains the proposed design method. Subsequently, the simulation study of designed PSSs is given in Section 4. Finally, the outcomes from this paper are summarized.

2. MOTIVATION OF THE PROPOSED CONTROL

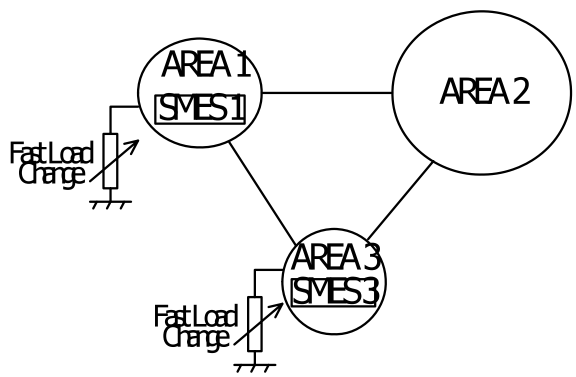

Fig. 1 Three-Area Loop Interconnected Power System with SMESs

A three-area loop interconnected power system [6] as shown in Fig. 1 is used as a study system. It is assumed the large loads with sudden change have been installed in areas 1 and 3. These load changes cause severe frequency oscillations in both areas. To solve this problem, SMES1 and SMES3 are placed in areas 1 and 3 respectively. Here, the frequency stabilizer of each SMES is designed by the proposed control.

3. PROPOSED CONTROL DESIGN

3.1 Coordinated Control of SMES and Governor

The response of SMES is extremely rapid when compared to the conventional frequency control system, i.e. a governor. The difference in responses signifies that the SMES and governor can be coordinated.

When a power system is subjected to a sudden load disturbance, the SMES quickly acts to damp frequency oscillation in the transient period. Subsequently, the governor continues to eliminate the steady-state error in frequency oscillation. As the periods of operation for the SMES and governor do not overlap, the dynamic of governor can then be neglected in the design of frequency stabilizer for the sake of simplicity.

3.2 Linearized Power System Model

The power system shown in Fig. 1 can be represented by a linearized power system model, as shown in Fig. 2. Note that the governors are eliminated in this system. The SMES model is represented by the active power controller [7]. The dynamic characteristic of SMES is modeled as the first order controller with a time constant $T_{SM} = 0.03$ sec. The linearized state equation of Fig. 2 can be expressed as:

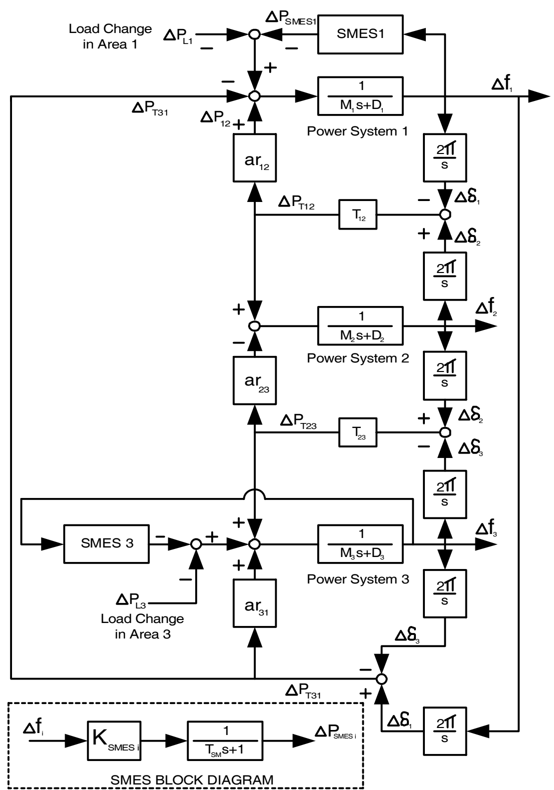

Fig. 2 Linearized Model of Three Area System for Control Design

$$S \ : \ \begin{bmatrix} \Delta\dot{f}_1 \\ \Delta\dot{P}_{T12} \\ \Delta\dot{f}_2 \\ \Delta\dot{P}_{T23} \\ \Delta\dot{f}_3 \end{bmatrix} = \begin{bmatrix} a_{11} & a_{12} & a_{13} & a_{14} & a_{15} \\ a_{21} & a_{22} & a_{23} & a_{24} & a_{25} \\ a_{31} & a_{32} & a_{33} & a_{34} & a_{35} \\ a_{41} & a_{42} & a_{43} & a_{44} & a_{45} \\ a_{51} & a_{52} & a_{53} & a_{54} & a_{55} \end{bmatrix} \begin{bmatrix} \Delta f_1 \\ \Delta P_{T12} \\ \Delta f_2 \\ \Delta P_{T23} \\ \Delta f_3 \end{bmatrix} + \begin{bmatrix} b_{11} & b_{12} \\ b_{21} & b_{22} \\ b_{31} & b_{32} \\ b_{41} & b_{42} \\ b_{51} & b_{52} \end{bmatrix} \begin{bmatrix} \Delta P_{SMES1} \\ \Delta P_{SMES2} \end{bmatrix} \tag{1}$$

where, a_{11} = $-D_1/M_1$, a_{12} = $(ar_{12}+T_{31}/T_{12})/M_1$, a_{14} = $-T_{31}/M_1T_{23}$, a_{21} = $-2\pi T_{12}$, a_{23} = $2\pi T_{12}$, a_{32} = $-1/M_2$, a_{33} = $-D_2/M_2$, a_{34} = $-ar_{23}/M_2$, a_{43} = $2\pi T_{23}$, a_{45} = $-2\pi T_{23}$, a_{52} = $-ar_{31}T_{31}/M_3T_{12}$, a_{54} = $(1+ar_{31}T_{31}/T_{23})/M_3$, a_{55} = $-D_3/M_3$, b_{11} = $-1/M_1$, b_{52} = $-1/M_3$, the others are equal to 0

The variable ΔP_{T31} is represented in terms of ΔP_{T12} and ΔP_{T23} by

$$\Delta P_{T31} = -\frac{T_{31}}{T_{12}}\Delta P_{T12} + \frac{T_{31}}{T_{23}}\Delta P_{T23} \tag{2}$$

Thus, ΔP_{T31} has disappeared in Eq. (1). This system has two conjugate pairs of complex eigenvalues and a negative real eigenvalue. The former corresponds to two inter-area oscillation modes and the latter the inertia center mode. Based on the mode controllability matrix, the inter-area modes between areas 1 and 2, and areas 2 and 3 are controllable for the control inputs ΔP_{SMES1} and ΔP_{SMES3}, respectively. Accordingly, the design purpose of frequency stabilizer is to enhance the damping of the mentioned inter-area modes.

3.3 Overlapping Decomposition

Since the system (1) is a Multi-Input Multi-Output (MIMO) system, it is not easy to design both frequency stabilizers simultaneously and directly from the system. To simplify the design process, the technique of overlapping decompositions [8-9] is applied to reduce the system (1) to a subsystem embedded with only the inter-area mode of interest. The original system (1) is referred to as the system S.

$$S : \begin{bmatrix} \dot{x}_1 \\ \dot{x}_2 \\ \dot{x}_3 \end{bmatrix} = \begin{bmatrix} A_{11} & A_{12} & A_{13} \\ A_{21} & A_{22} & A_{23} \\ A_{31} & A_{32} & A_{33} \end{bmatrix} \begin{bmatrix} x_1 \\ x_2 \\ x_3 \end{bmatrix} + \begin{bmatrix} B_{11} & B_{12} \\ B_{21} & B_{22} \\ B_{31} & B_{32} \end{bmatrix} \begin{bmatrix} u_1 \\ u_2 \end{bmatrix} \tag{3}$$

The sub-matrices A_{ij} and B_{ij}, $(i, j = 1, 2, 3)$ have appropriate dimensions identical to the corresponding states and input vectors. According to the process of overlapping decompositions, the system S can be expressed as:

$$\tilde{S} : \begin{bmatrix} \dot{z}_1 \\ \dot{z}_2 \end{bmatrix} = \begin{bmatrix} A_{11} & A_{12} & 0 & A_{13} \\ A_{21} & A_{22} & 0 & A_{23} \\ A_{21} & 0 & A_{22} & A_{23} \\ A_{31} & 0 & A_{32} & A_{33} \end{bmatrix} \begin{bmatrix} z_1 \\ z_2 \end{bmatrix} + \begin{bmatrix} B_{11} \\ B_{21} \\ B_{21} \\ B_{31} \end{bmatrix} \begin{bmatrix} u_1 \\ u_2 \end{bmatrix} \tag{4}$$

where $z_1 = \left[x_1^T, x_2^T\right]^T$ and $z_2 = \left[x_2^T, x_3^T\right]^T$. Subsequently, the system $\tilde{S}$ can be decomposed into two interconnected overlapping subsystems, i.e.

$$\begin{aligned}\tilde{S}_1 \;:\; \dot{z}_1 &= \left(\begin{bmatrix} A_{11} & A_{12} \\ A_{21} & A_{22} \end{bmatrix} z_1 + \begin{bmatrix} B_{11} \\ B_{21} \end{bmatrix} u_1\right) \\ &+ \begin{bmatrix} 0 & A_{13} \\ 0 & A_{23} \end{bmatrix} z_2 + \begin{bmatrix} B_{12} \\ B_{22} \end{bmatrix} u_2 \end{aligned} \tag{5}$$

and

$$\begin{aligned}\tilde{S}_2 \;:\; \dot{z}_2 &= \left(\begin{bmatrix} A_{22} & A_{23} \\ A_{32} & A_{33} \end{bmatrix} z_2 + \begin{bmatrix} B_{21} \\ B_{31} \end{bmatrix} u_2\right) \\ &+ \begin{bmatrix} A_{21} & 0 \\ A_{31} & 0 \end{bmatrix} z_1 + \begin{bmatrix} B_{21} \\ B_{31} \end{bmatrix} u_1 \end{aligned} \tag{6}$$

The state variable x_2 is repeatedly included in both subsystems, which implies "Overlapping Decompositions".

For system stabilization, two interconnected subsystems $\tilde{S}_1$ and $\tilde{S}_2$ are considered. The terms in the right hand sides of Eqs. (5) and (6) can be separated into the decoupled subsystems (as indicated in the parenthesis in Eqs. (5) and (6)) and the interconnected subsystems. As mentioned in [8-9], if each decoupled subsystem can be stabilized by its own input, the asymptotic stability of the interconnected overlapping subsystem and and are maintained. Moreover, the asymptotic stability of the original system is also guaranteed. Consequently, the interactions of the decoupled subsystems with the interconnection subsystems in Eqs. (5) and (6) are regarded as perturbations. They can be neglected during control design. As a result, the decoupled subsystems of Eqs. (5) and (6) can be expressed as:

$$\tilde{S}_{D1} \;:\; \dot{z}_1 = \begin{bmatrix} A_{11} & A_{12} \\ A_{21} & A_{22} \end{bmatrix} z_1 + \begin{bmatrix} B_{11} \\ B_{21} \end{bmatrix} u_1 \tag{7}$$

and $$\tilde{S}_{D2} \;:\; \dot{z}_2 = \begin{bmatrix} A_{22} & A_{23} \\ A_{32} & A_{33} \end{bmatrix} z_2 + \begin{bmatrix} B_{22} \\ B_{32} \end{bmatrix} u_2 \tag{8}$$

By regarding the power deviation between areas 1 and 2 (ΔP_{T12}) as the overlapped variable for design of frequency stabilizer of SMES1, the subsystem embedded with the inter-area mode between areas 1 and 2 can be expressed as:

$$\begin{aligned}\tilde{G}_{s1} \;:\; \begin{bmatrix} \Delta\dot{f}_1 \\ \Delta\dot{P}_{T12} \end{bmatrix} &= \begin{bmatrix} -D_1/M_1 & \left(ar_{12} + T_{31}/T_{12}\right)/M_1 \\ -2\pi T_{12} & 0 \end{bmatrix} \begin{bmatrix} \Delta f_1 \\ \Delta P_{T12} \end{bmatrix} \\ &+ \begin{bmatrix} 1/M_1 \\ 0 \end{bmatrix} \Delta P_{SMES1} \end{aligned} \tag{9}$$

Next, by considering the power deviation between areas 2 and 3 (ΔP_{T23}) as the overlapped variable for design of frequency stabilizer of SMES3, the subsystem embedded with the inter-area mode between areas 2 and 3 can be expressed as:

$$\tilde{G}_{s2} \;:\; \begin{bmatrix} \Delta \dot{P}_{T23} \\ \Delta \dot{f}_3 \end{bmatrix} = \begin{bmatrix} 0 & -2\pi T_{23} \\ 1 + a_{31}T_{31}/T_{23}/M_3 & -D_3/M_3 \end{bmatrix} \begin{bmatrix} \Delta P_{T23} \\ \Delta f_3 \end{bmatrix} + \begin{bmatrix} 0 \\ -1/M_3 \end{bmatrix} \Delta P_{SMES3} \tag{10}$$

Eqs. (9) and (10) are used to design SMES1 and SMES3, respectively. It should be noted that after the process of overlapping decompositions, the original MIMO system (1) are divided into two decoupled Single-Input Single-Output (SISO) subsystems (Eqs. (10) and (11)). Accordingly, each frequency stabilizer can be independently designed in the decoupled subsystem.

3.4 H_∞ Control Design

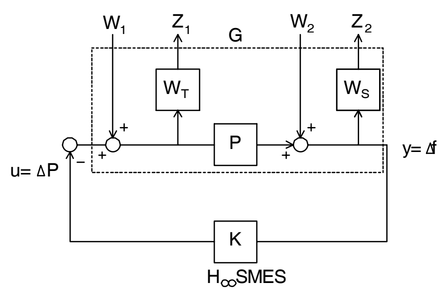

Fig. 3 H_∞ control design

In order to design the controller based on H_∞ method, each decoupled subsystem can be formulated into Linear Fractional Transformation model in Fig. 3 [10]. The multificative uncertainty is used to model all possible perturbed plants. For the system notations, P is the interconnected system which consists of nominal plant G, i.e., a transfer function of a decoupled subsystem, performance weighting function W_S and uncertainties weighting function W_T, y is a measurement plant output, u is a control signal, w_1 and w_2 are disturbances at plant input and output, respectively, z_1 and z_2 are error signals of W_T and W_S weights, respectively. The H_∞ controller is represented by controller K. It utilizes the frequency deviation Δf_i of the controlled area as the feedback signal input.

To achieve robustness, the controller must be obtained satisfying inequality (11) and (12) for the control system

$$\|S\|_\infty \le \left\|W_S^{-1}\right\|_\infty \tag{11}$$

$$\|T\|_\infty \le \left\|W_T^{-1}\right\|_\infty \tag{12}$$

where, S is the sensitivity transfer function $((I+GK)^{-1})$ and T is the complementary sensitivity transfer function $(GK(I+GK)^{-1})$. According to inequalities (11) and (12), The W_S is selected in form of low pass filter as:

$$W_S = \frac{s+5}{2s+5} \tag{13}$$

For all frequencies, the relation of $S + T = I$ is held. Thus, W_T is selected in form of high pass filter as:

$$W_T = \frac{s+3}{s+10} \tag{14}$$

As a result, the H_∞-based frequency stabilizer of SMES in an area 1 is

$$K_{SMES\ 1} = \frac{34s^3 + 781s^2 + 1379s - 157}{s^4 + 129s^3 + 1279s^2 + 2473s + 159} \tag{15}$$

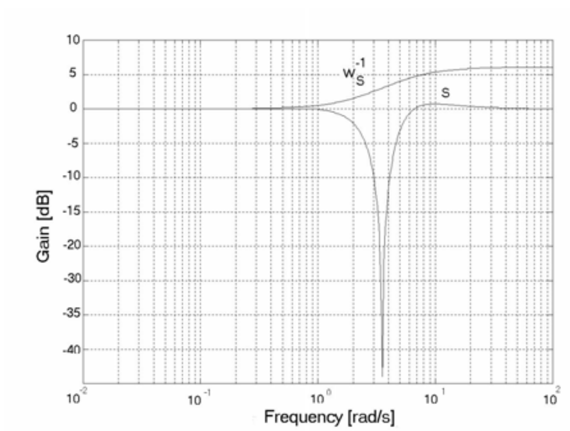

Fig. 4 Bode Plot of S and W_S^{-1}

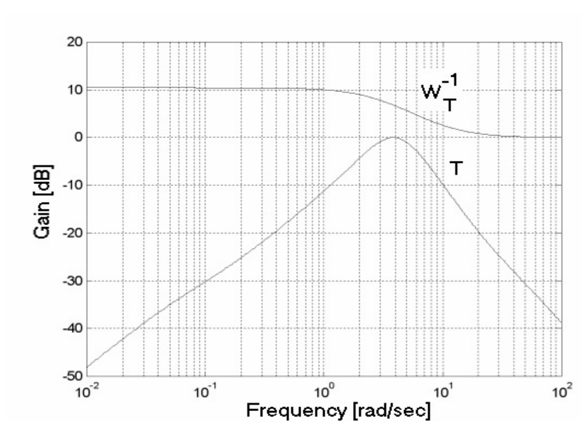

Fig. 5 Bode Plot of T and W_T^{-1}

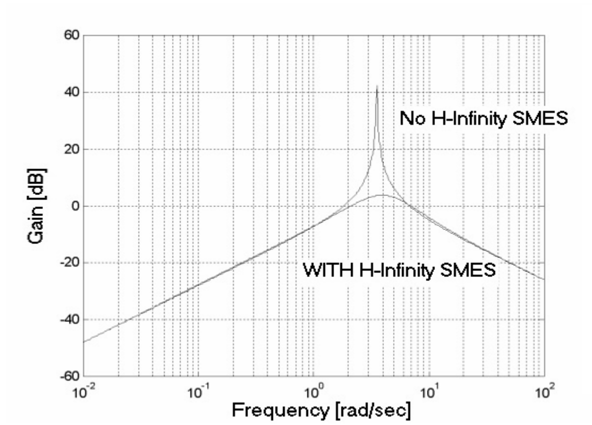

Fig. 6 Bode Plot of subsystem (9) (Before and After Applying H_∞ SMES)

Fig. 4 and Fig. 5 confirm that the conditions in inequalities. (11) and (12) are satisfied by the designed controller K_{SMES1}. In addition, the control effect of H_∞-based stabilizer is clearly shown by bode plots of designed model in Fig. 6. The H_∞-based stabilizer is capable of reducing the peak resonance in the frequency of inter-area oscillation mode.

The same strategy is used to design the H_∞-based stabilizer in area 3. W_S and W_T are selected as:

$$w_S = \frac{s+10}{2s+20} \tag{16}$$

$$w_T = \frac{s+4}{s+10} \tag{17}$$

As a result, the H_∞-based frequency stabilizer of SMES in area 3 is given by:

$$K_{SMES3} = \frac{193S^3 + 3800S^2 + 13869s - 842}{s^4 + 422s^3 + 5586s^2 + 17645s + 678} \tag{18}$$

4. SIMULATION RESULTS

In simulation, the designed H_∞-based stabilizer is compared to the PID-based frequency stabilizer. Based on the same first overshoot of frequency oscillation against 0.01 pu.MW step load increase in areas 1 and 3, The PID-based stabilizer are given as:

$$K_{SMES1} = 0.07 + \frac{1}{s} + 0.05s \tag{19}$$

$$K_{SMES3} = 0.15 + \frac{1}{s} + 0.10s \tag{20}$$

In addition, the governor is included in a linearized power model in a simulation study, as shown in Fig. 7.

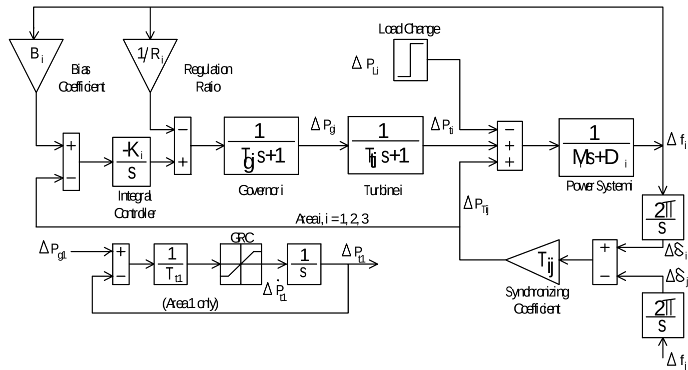

Fig. 7 Linearized model with governor

Simulation studies are separated to 3 cases as shown in Fig. 8.

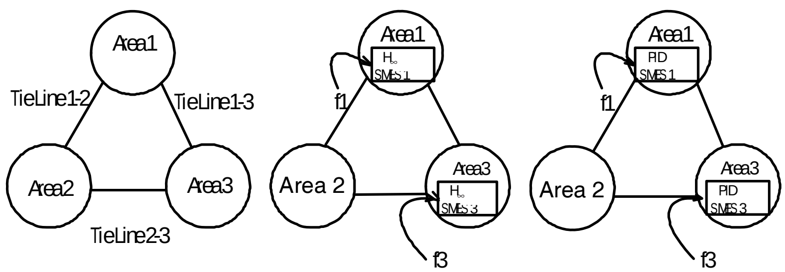

Fig. 8 Case studies for Three Area Loop System

Figs. 9 and 10 show the dynamics responses for 0.01 pu.MW step load disturbance in areas 1 and 3. H_∞-based stabilizers provide better damping effects on frequency oscillations Δf_1 and Δf_3 than those of PID-based stabilizers.

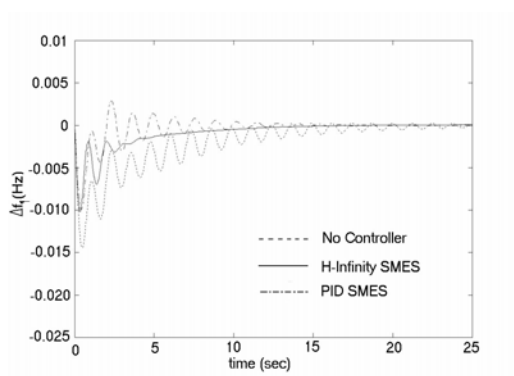

Fig. 9 Frequency Deviation of Area 1

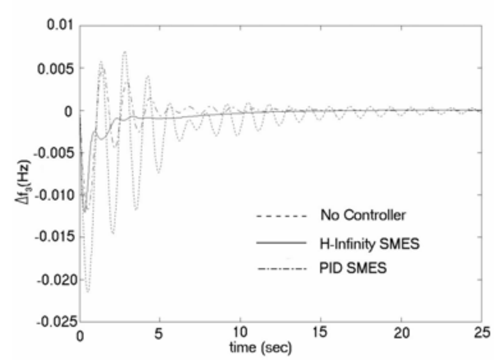

Fig. 10 Frequency Deviation of Area 3

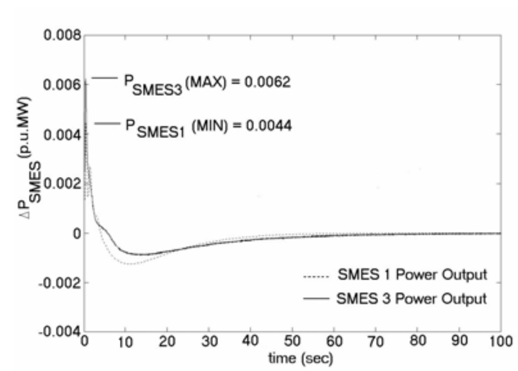

Fig. 11 The active power output of H_∞ - based stabilizer

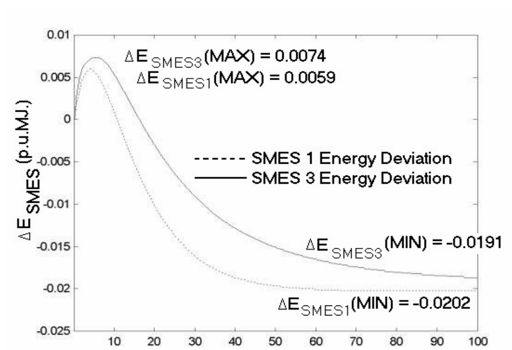

Fig. 12 The energy deviations of H_∞ - based stabilizer

Fig. 11 shows the active power outputs of H_∞ - based stabilizers. The MW capacities of SMES are evaluated from the peak value of power output of the SMES. The MW capacities of SMES1 and SMES3 are 0.0044 and 0.0062 pu.MW, respectively. Fig. 12 shows the MJ energy deviations of H_∞ - based stabilizers that evaluated from

$$\Delta E_{SMES} = \int \Delta P_{SMES}\, dt \tag{21}$$

Necessary MJ capacity of SMES can be calculated by:

$$MJ\ Capacity = \Delta E_{SMES(MAX)} - \Delta E_{SMES(MIN)} \tag{22}$$

As a result, MJ capacities of SMES1 and SMES3 are 0.0261 and 0.0265 pu. MJ, respectively.

Next, the load changes appiled to areas 1 and 3 are assumed to be $\Delta P_{L1} = -0.002 \sin(3t) + 0.004 \sin(6t) - 0.007 \sin(9t)$ and $\Delta P_{L3} = -0.001 \sin(1t) + 0.004 \sin(5t) - 0.005 \sin(7t)$, respectively. Suppose that the system is in unstable state so that the system damping coefficient D_1 and D_3 are -0.3 [pu.MW/Hz]. As shown in Figs. 13 and 14, the power system with PID-based stabilizer completely loses stability, frequency oscillations in areas 1 and 3 severely fluctuate and finally diverge. On the other hand, frequency oscillations are effectively stabilized by H_∞-based stabilizers. These results confirm that the robustness of the H_∞-based stabilizer is superior to that of the PID-based stabilizer.

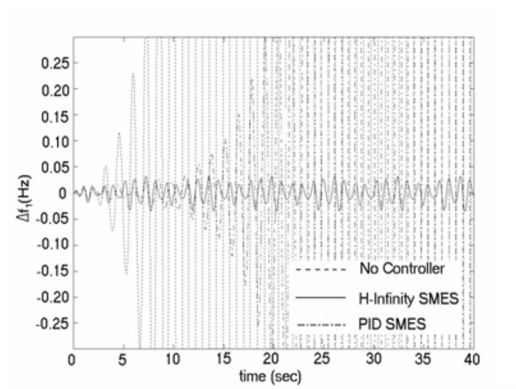

Fig. 13 Frequency Deviation of Area 1

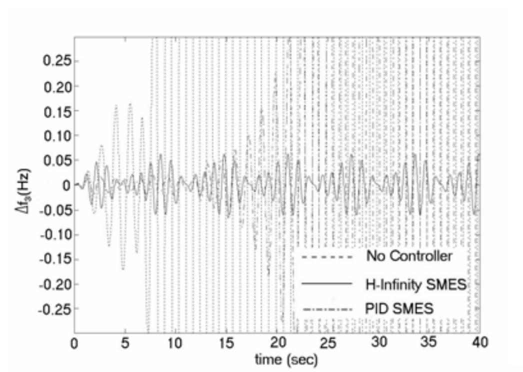

Fig. 14 Frequency Deviation of Area 3

5. CONCLUSIONS

This paper focuses on the new robust design of frequency stabilizer of SMES by taking system uncertainties into consideration. The overlapping decompositions technique is used to extract the SISO subsystem embedded with the inter-area oscillation mode of interest from the original MIMO system. As a result, each frequency stabilizer can be independently designed in the decoupled subsystem. By including the multiplicative uncertainty model in the decoupled subsystem, the H_∞ control via mixed sensitivity approach can be applied to design frequency stabilizer of SMES. The resulted H_∞ frequency stabilizer is low order controller. In addition, it used only a frequency deviation of the control area as a local signal input. Experimental studies have confirmed the high robustness of the designed frequency stabilizers against various load disturbances with changing frequency in the vicinity of inter-area mode and negative damping.

6. REFERENCES

[1] Jaleeli. 1992. Understanding Automatic Generation Control. *IEEE Trans. on Power System* 7(3): 1106-1112.

[2] Hassenzahl, W. 1989. Superconducting Magnetic Energy Storage. *IEEE Trans. on Magnetics* 25(2): 750-758.

[3] Banerjee, S.; Chatterjee, J.K.; and Tripathy, S.C. 1990. Application of Magnetic Energy Storage Unit as Load-Frequency Stabilizer. *IEEE Trans. on Energy Conversion* 5(1): 46-51.

[4] Tripathy, S.C. and Juengst, K.P. 1997. Sampled Data Automatic Generation Control with Superconducting Magnetic Energy Storage in Power Systems. *IEEE Trans. on Energy Conversion* 12(2): 187-192.

[5] Tripathy, S.C.; Balasubramanian, R.; and Chandramohanan Nair, P.S. 1992. Effect of Superconducting Magnetic Energy Storage on Automatic Generation Control Considerating Governor Deadband and Boiler Dynamics. *IEEE Trans. on Power System* 7(3): 1266-1273.

[6] Elgerd, O.L. 1985. *Electric Energy System Theory*. An Introduction. 2nd edition: McGraw-Hill, 340 p.

[7] Mitani, Y.; Tsuji, K.; and Murakami, Y. 1998. Application of Superconducting Magnetic Energy Storage to Improve Power System Dynamics Performance. *IEEE Trans. On Power System* 3(4): 1418-1425.

[8] Singh, M.G. 1981. *Decentralised Control*. North-Holland Systems and Control Series: 322-327.

[9] Ikeda, M. et al. 1981. Decentralized control with overlapping information sets. *Journal of Optimization Theory and Applications* 34(2): 279-310.

[10] Zhou, K. 1998. *Essentials of Robust Control*: Prentice-Hall, Inc.